



Alternating wet and dry depositional environments recorded in the stratigraphy of Mount Sharp at Gale crater, Mars

W. Rapin, G. Dromart, D. Rubin, Laetitia Le Deit, Nicolas Mangold, L.A. Edgar, Olivier Gasnault, K. Herkenhoff, Stéphane Le Mouélic, R.B. Anderson, et al.

► To cite this version:

W. Rapin, G. Dromart, D. Rubin, Laetitia Le Deit, Nicolas Mangold, et al.. Alternating wet and dry depositional environments recorded in the stratigraphy of Mount Sharp at Gale crater, Mars. *Geology*, 2021, 10.1130/G48519.1 . insu-03198811

HAL Id: insu-03198811

<https://insu.hal.science/insu-03198811>

Submitted on 15 Apr 2021

HAL is a multi-disciplinary open access archive for the deposit and dissemination of scientific research documents, whether they are published or not. The documents may come from teaching and research institutions in France or abroad, or from public or private research centers.

L'archive ouverte pluridisciplinaire **HAL**, est destinée au dépôt et à la diffusion de documents scientifiques de niveau recherche, publiés ou non, émanant des établissements d'enseignement et de recherche français ou étrangers, des laboratoires publics ou privés.



Distributed under a Creative Commons Attribution - NoDerivatives 4.0 International License

Alternating wet and dry depositional environments recorded in the stratigraphy of Mount Sharp at Gale crater, Mars

W. Rapin^{1,2,3}, G. Dromart⁴, D. Rubin⁵, L. Le Deit⁶, N. Mangold⁶, L.A. Edgar⁷, O. Gasnault¹, K. Herkenhoff⁷, S. Le Mouélic⁶, R.B. Anderson⁷, S. Maurice¹, V. Fox³, B.L. Ehlmann^{3,8}, J.L. Dickson³ and R.C. Wiens⁹

¹Institut de Recherche en Astrophysique et Planétologie, Université de Toulouse, CNRS, CNES, 31400 Toulouse, France

²Institut de Minéralogie, de Physique des Matériaux et de Cosmochimie (IMPMC), Sorbonne Université, CNRS, 75006 Paris, France

³Division of Geological and Planetary Sciences, California Institute of Technology, Pasadena, California 91125, USA

⁴Laboratoire de Géologie de Lyon Terre Planètes Environnement, Université de Lyon, 69364 Lyon, France

⁵Department of Earth and Planetary Sciences, University of California, Santa Cruz, California 95064, USA

⁶Laboratoire de Planétologie et Géodynamique, Université de Nantes, CNRS, 44300 Nantes, France

⁷Astrogeology Science Center, U.S. Geological Survey, Flagstaff, Arizona 86001, USA

⁸Jet Propulsion Laboratory, Pasadena, California 91109, USA

⁹Los Alamos National Laboratory, Los Alamos, New Mexico 87545, USA

ABSTRACT

The Curiosity rover is exploring Hesperian-aged stratigraphy in Gale crater, Mars, where a transition from clay-bearing units to a layered sulfate-bearing unit has been interpreted to represent a major environmental transition of unknown character. We present the first description of key facies in the sulfate-bearing unit, recently observed in the distance by the rover, and propose a model for changes in depositional environments. Our results indicate a transition from lacustrine mudstones into thick aeolian deposits, topped by a major deflation surface, above which strata show architectures likely diagnostic of a subaqueous environment. This model offers a reference example of a depositional sequence for layered sulfate-bearing strata, which have been identified from orbit in other locations globally. It differs from the idea of a monotonic Hesperian climate change into long-term aridity on Mars and instead implies a period characterized by multiple transitions between sustained drier and wetter climates.

INTRODUCTION

Gale crater on Mars, currently being explored by the Mars Science Laboratory (MSL) Curiosity rover, belongs to a family of impact craters referred to as “overfilled” (Grotzinger and Milliken, 2012; Bennett and Bell, 2016) with kilometer-thick exposures of layered fill approaching or even exceeding the crater rim elevation. Gale preserves a 5-km-thick sequence of stratified rocks expressed today as a partially eroded mound, informally named Mount Sharp, offering an extended record of paleoenvironments (Fig. 1). From orbit, the lowermost section has been dated to the Hesperian (3.61 ± 0.06 Ga; Le Deit et al., 2013) and exhibits spectral signatures of clay minerals transitioning upward to sulfates over a stratigraphic height of ~ 300 m (Milliken et al., 2010; Fraeman et al., 2016). Investigating this change in mineralogy, which may record a ma-

ior environmental transition characteristic of strata across Mars (Bibring et al., 2006), is one of the primary objectives of the Curiosity rover mission (Grotzinger et al., 2012).

To date, the rover has analyzed the clay-bearing lacustrine deposits of the Murray formation at the base of Mount Sharp, and is currently just below the thicker interval referred to as the layered sulfate-bearing unit (LSu) (Fraeman et al., 2016; Fig. 1). In the northwest portion of Mount Sharp, including the planned rover traverse region, the LSu covers ~ 700 m in elevation and constitutes the uppermost unit of the Mount Sharp group (Grotzinger et al., 2015). Orbital High Resolution Imaging Science Experiment (HiRISE, aboard Mars Reconnaissance Orbiter) images showed that the LSu is composed of subparallel strata that vary in albedo, surface texture, and thickness from decameter to meter scale (Stack et al., 2013).

The lower LSu, to a height of ~ 150 m from the base, is topped by a distinctive layer referred to as the marker bed (Fig. 1), initially identified as a thin, smooth, low-albedo layer mapped regionally for 75 km across Mount Sharp (Milliken et al., 2010). The marker bed is pyroxene-bearing and lacks spectral signatures of sulfate in orbital data (Powell et al., 2019). Hydrated Mg-sulfate signatures occur in the section just beneath the marker bed and throughout the section above (Milliken et al., 2010; Fraeman et al., 2016; Fig. 1).

We report the first ground-based rover observations of bedding structures, textures, and stratigraphic architectures throughout the LSu using the Remote Micro-Imager (RMI) of the ChemCam instrument (Le Mouélic et al., 2015), the first ground-based images resolving bedding structures throughout the LSu. We provide an analysis of the stratal components and sedimentary structures at outcrop scale and the highest available resolution. We then propose a model for depositional systems and their evolution in the sulfate-bearing unit that can be tested in situ with further data collection by the Curiosity rover, and describe implications for layered sulfate-bearing terrains elsewhere on Mars.

DATASET AND METHODS

The ChemCam panchromatic RMI provides context images for chemical analyses at stand-off distances of a few meters, but it can also be used for imaging features as far as several

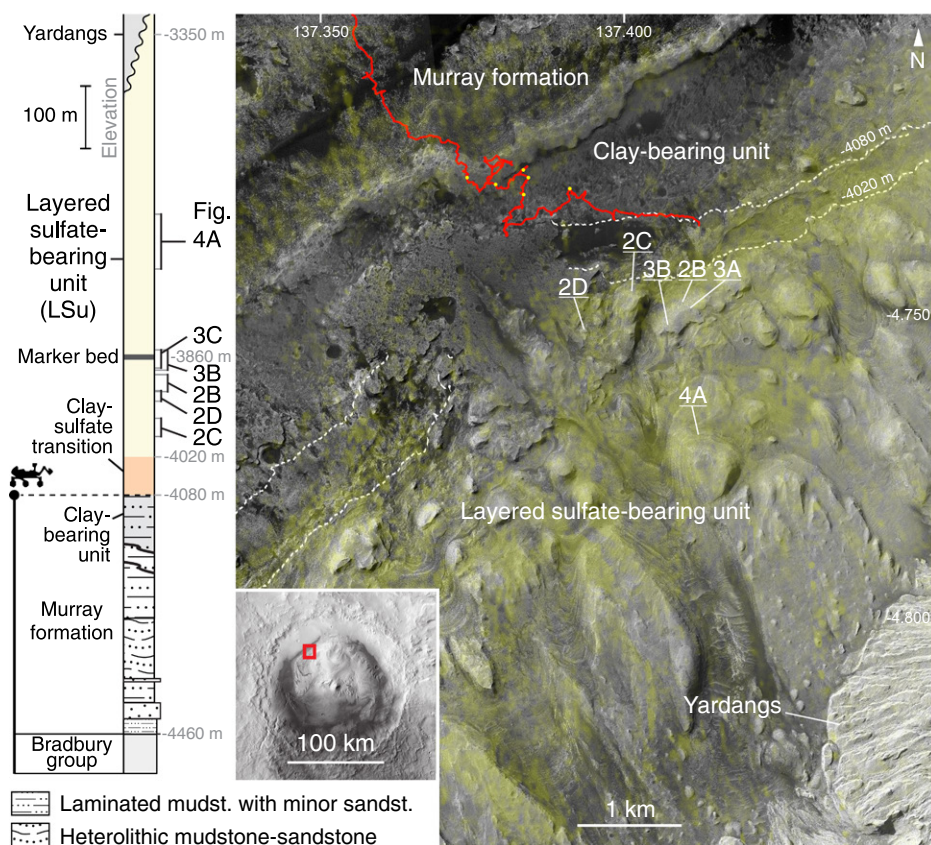


Figure 1. Stratigraphic column (left) of the base of Mount Sharp, Mars, represents the elevation of units (see Table S2 [see footnote 1]) with sections covered by images of outcrops from Figures 2–4. Map (right) shows NASA Curiosity rover traverse (red), along with locations from which Remote Micro-Imager images were acquired (yellow dots), on the High Resolution Imaging Science Experiment (HiRISE) base map overlaid with Compact Reconnaissance Imaging Spectrometer for Mars (CRISM) S-index, which tracks sulfates (shaded yellow). Elevation contours of sulfate-clay transition (white dotted lines) and positions of outcrops from Figures 2–4 are also shown.

kilometers away (Le Mouélic et al., 2015). It offers the finest resolution of the Curiosity's remote-sensing cameras, an essential capability for observing distant sedimentary structures (Fig. S1 in the Supplemental Material¹). The smallest discernable details are 6–10 cm at 1 km distance and 30–50 cm at 5 km distance in the best focus conditions (Le Mouélic et al., 2015). Beyond 5 km, the spatial resolution of HiRISE is better than that of the RMI, yet the two are complementary by offering orthogonal viewing angles. While it was not originally designed for this purpose, the RMI has been demonstrated to be a powerful scouting tool, with best performance using a new autofocus algorithm (Gasnault et al., 2016).

Mosaics were produced from individual RMI images acquired with spacing (8–10 mrad)

ensuring overlap to form a contiguous view of the target. The images were processed with dark and flat field corrections then stitched, denoised, and slightly sharpened for small-scale contrasts (Le Mouélic et al., 2019). Using a GIS visibility analysis, mosaics were integrated with the HiRISE stereo digital elevation model (DEM) (Kirk et al., 2008) as projected viewsheds to allow location of the observed outcrops on the stratigraphic column (Fig. S2; Fig. 1).

RESULTS AND INTERPRETATIONS

The imaging campaign covered key outcrops of the LSu (Fig. 1), divided into (1) a lower part below and including the marker bed (Figs. 2 and 3; massive looking), observed at 1.5–2.5 km distance; and (2) an upper part above the marker bed (Fig. 4; heterolithic bedding), observed at 3–5 km distance. Imaging of the LSu within the clay-sulfate transition interval (Fig. 1) has so far been precluded by viewing geometry. Image acquisition was driven by the opportunistic visibility of outstanding outcrops as the rover traversed upward onto the slopes of Mount Sharp.

Large-Scale Aeolian Cross-Bedding in the Lower Unit

The lowest visible LSu interval exhibits large-scale trough and planar cross-bedding. Figure 2 shows sets dipping in different directions that are bounded by erosive surfaces. The thickness of the cross-bedded sets (5–10 m) and lack of morphological evidence for channels support deposition by migrating aeolian dunes and preclude a subaqueous origin. Requiring typical flow depths of at least 6× dune height (Bradley and Venditti, 2017), only a fraction of which is typically preserved by the bedsets, a fluvial origin is likely not suitable to the context of Gale crater. A particular facies with wavy, uniformly spaced beds with decameter-scale wavelength is also observed (Fig. 2B). These patterns are also likely of aeolian origin due to their scale. They are consistent with laterally shifting superimposed lee-side spurs common to aeolian cross-strata (Rubin and Carter, 2006, their figures 46d–46f). Their high degree of preservation implies a locally high accumulation rate on the dunes' lee side.

Clear tabular cross-bedding associated with sand sheet strata has not been identified; structures correspond instead to trough cross-bedding formed by superimposed dunes migrating in different directions (Fig. S4). Outcrops as much as 3 km away laterally exhibit cross-bedded structures of similar scale (Fig. S5), which suggests the aeolian system is extensive within this interval. Aeolian cross-stratification has also been reported locally in orbital data on other parts of Mount Sharp (Milliken et al., 2014). Correlations between orbital and ground-based observations on scattered regional outcrops is challenging, but these independently support multiple episodes of aeolian deposition.

The Marker Bed as a Major Deflationary Surface

The marker bed is a regionally extensive, dark-toned layer distinguishable from orbit and now observed in cross-sectional view at higher resolution (Fig. 3). The marker bed is characterized by a variably prominent, few-meters-thick, resistant lip. Its exposure marks the upper boundary of the cross-bedded strata package (Fig. 2A). It is relatively flat on the outcrop scale, but its basal boundary surface presents significant irregularities at smaller scale, locally cutting across underlying strata (Fig. 3).

Textures on the marker bed lip are heterogeneous with lens-shaped zones of blocky texture, but the blocks themselves are homogeneous in albedo and texture; there are no apparent exotic blocks in a mélange. Some blocks are 2 m in size and show subhorizontal bedding similar to that in underlying strata. These observations collectively hint at disruption within the forma-

¹Supplemental Material. Additional tables of stratigraphic elements, and close-up figures highlighting more details on RMI images. Please visit <https://doi.org/10.1130/G48519.1/5274996/g48519.pdf> to access the supplemental material, and contact editing@geosociety.org with any questions.

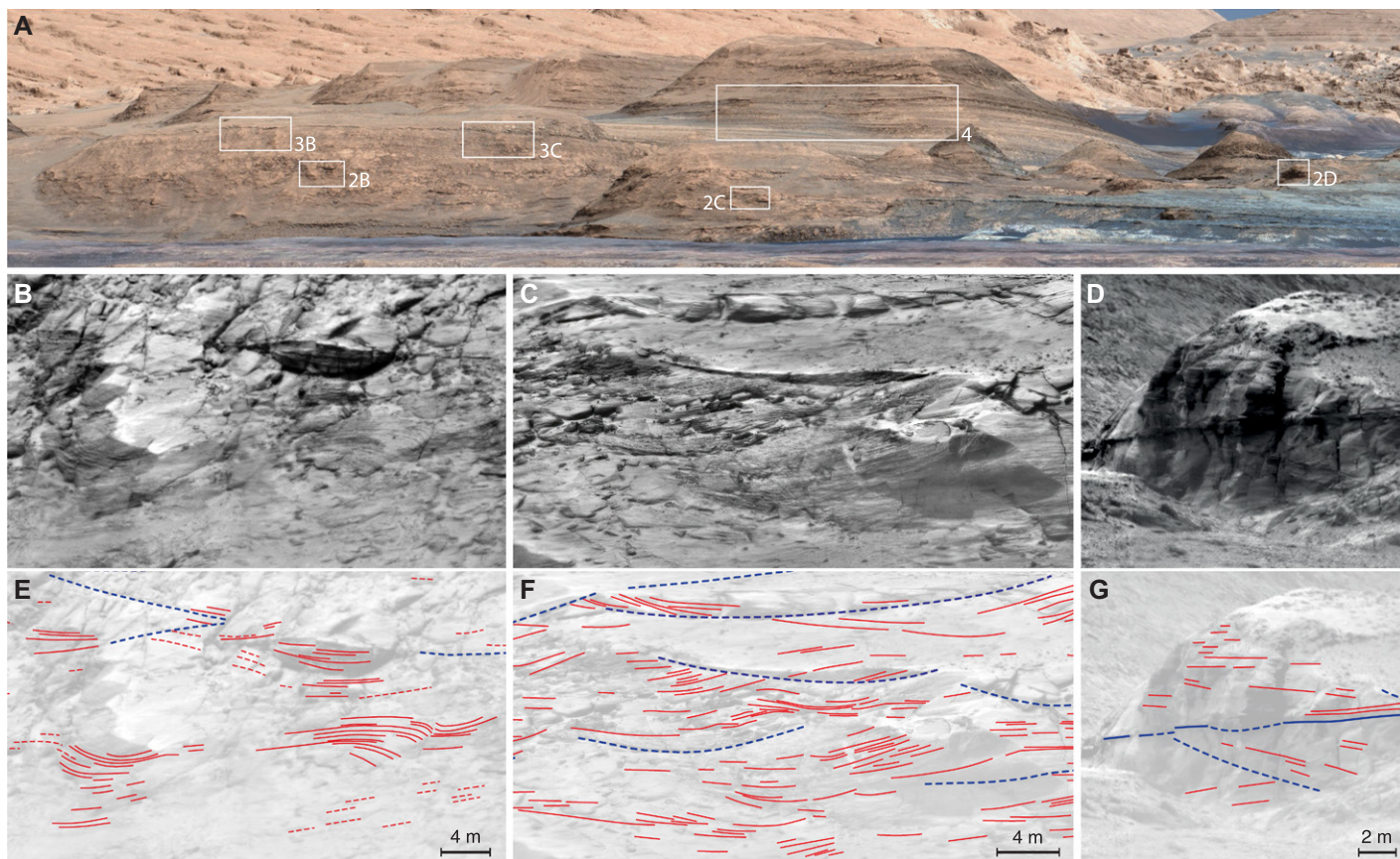


Figure 2. (A) NASA Curiosity Rover Mastcam mosaic covering buttes (image mcam06060) with locations of Remote Micro-Imager (RMI) images from Figures 2–4 (white boxes). (B–G) RMI mosaics showing sedimentary structures consistent with aeolian cross-bedding (B–D) with tracing overlay (E–G) of sets of cross-strata (red) and bounding surfaces (dark blue), including wavy (B, E: sol 2435 [sol—Mars solar day], ccam03435) and trough cross-bedding (C, F: sol 2396, ccam04395; D, G: sol 2295, ccam02295). Candidate bounding surface lines are dashed where clear identification is challenging. (See larger RMI images in Fig. S3 [see footnote 1]).

tion. The stratigraphic context, i.e., top of an aeolian sequence, disfavors subaerial or subaqueous gravity-related deposits. Instead, in this context, such textural and geometric features are typical of a super bounding surface (Kocurek, 1988), a type of hiatal surface common to terrestrial aeolian strata marking a break in dune development (Loope, 1985; Scherer, 2000; Mauz et al., 2013). The prevalence of near-horizontal planar beds in the uppermost aeolian sequence below the marker bed (Fig. 3) might point to the decrease in sedimentation rate that would be expected to have preceded such a hiatus resulting in thinner horizontal sets of strata. The blocky texture on the marker bed lip could be the result of amalgamated deflation surfaces forming a lag deposit, and/or breccias produced by shallow dissolution collapse of sulfate-cemented sandstones.

Extensive super surfaces of interior basins represent termination of dune fields due to uplift, dune migration, or climate change (Kocurek, 1988). Uplift and/or dune migration tend to generate planar deflationary surfaces, whereas a shift to wetter conditions can produce crusts, lags, and meter-scale irregularities (Kocurek, 1988). With the irregularities of the surface and

lip texture indicating a possible lag (Figs. 3B and 3C), the climate-change hypothesis appears most likely.

A Fluvial Depositional System for the Upper Stratified Unit

Above the marker bed, the layering in the LSu is visible in HiRISE imagery in the form of decameter-thick, cliff-forming planar beds or groups of beds. From orbit, layers are characterized by variegated tonality from dark to light toned, with some layers limited to tens or hundreds of meters in lateral extent. From the ground, the RMI view reveals stratal bifurcations, interruptions, or wedging (Fig. 4).

Within the outcrop, three facies are discriminated (Fig. 4): (1) erosion-resistant, variably massive bodies; (2) sets of interbedded recessive and erosion-resistant lithologies (i.e., heterolithic facies; Figs. 4B–4D); and (3) recessive and variably toned intervals. Along the Curiosity rover traverse explored so far, erosion-resistant outcrops of similar scale range from conglomeratic to fine-sandstone lithofacies, and recessive intervals are composed of mudstones (e.g., Edgar et al., 2018; Stack et al., 2018). We hypothesize outcrops within the LSu fol-

low this lithological pattern and, based on evidence from stratal architectures and textures, therefore likely represent (1) sandstone facies, (2) heterolithic facies, and (3) mudstone facies. Lens-shaped sandstone bodies embedded in mudstone lithologies (Fig. 4E) are not consistent with the geometry of aeolian sand sheets and dunes. Instead, the depositional architectures observed likely reflect a wetter environment. While local prograding sandstone beds (Fig. 4E, lower right) could point to a pro-deltaic environment, we propose that our observations are collectively best interpreted as a fluvial facies tract with channel, banks, levees, and floodplain deposits.

In this model, heterolithic intervals would represent sheet-like crevasse splays, and recessive mudstones would represent a floodplain environment distant from active channel influences. The sandstone bodies show a variety of geometries, laterally restricted and wing shaped, including sheet-like (width to depth ratio >15) and thicker ribbon-like bodies (Gibling, 2006). Some of these sandstone bodies form variably massive ridges that could correspond to fluvial levees. The exposed general stacking pattern of the sandstones, staggered obliquely and not

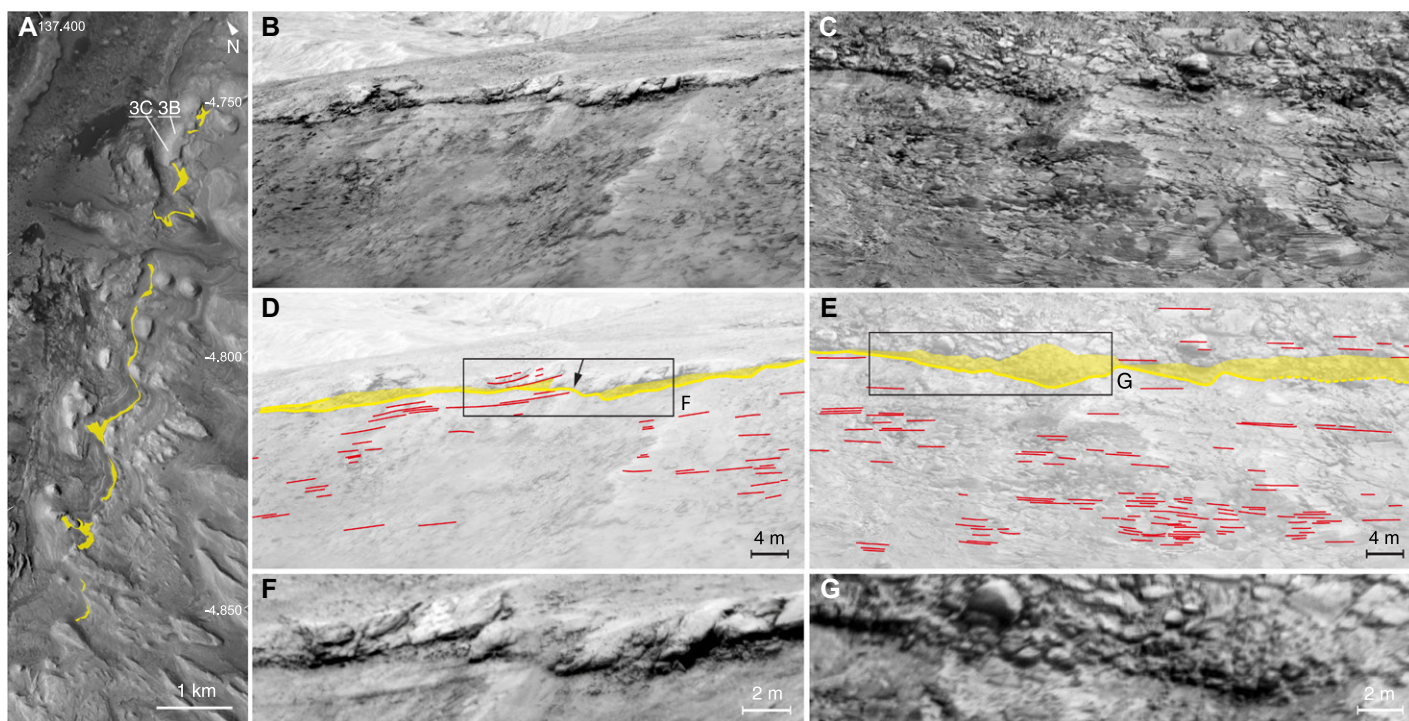


Figure 3. (A) High Resolution Imaging Science Experiment (HiRISE) map of exposed marker bed surface of Mount Sharp, Mars, highlighted in yellow. (B–G) Remote Micro-Imager (RMI) mosaics with tracing overlay (see context in Fig. 2A) showing meter-thick, erosion-resistant lip at the elevation of the marker bed (B,D: sol 2461 [sol—Mars solar day], image ccam04461; C, E: sol 2852, ccam04851), with visible bedding (red) and blocky textures at meter to sub-meter scale (shaded yellow), forming an irregular bounding surface (yellow) that locally cross-cuts bedding below (e.g., arrow in D). Enlarged views highlight textures and cross-cutting relationship (F,G; see also larger RMI images in Fig. S6 [see footnote 1]).

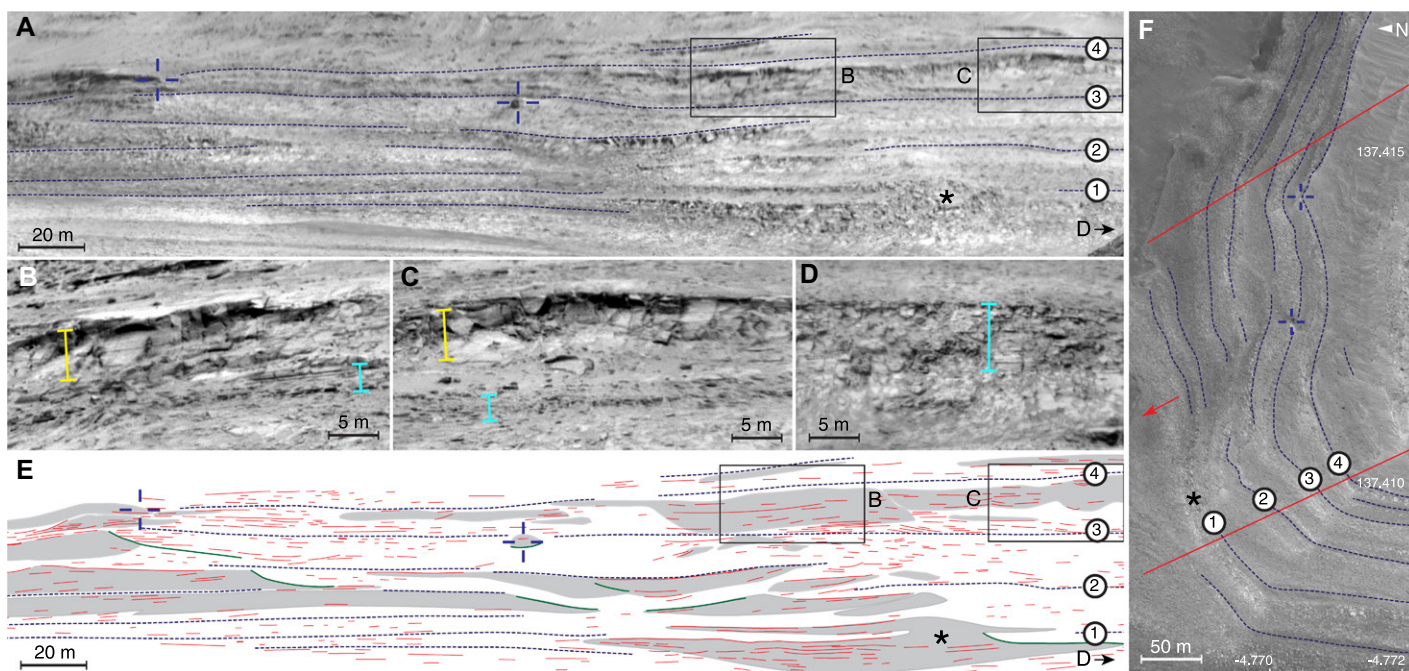


Figure 4. (A) Remote Micro-Imager (RMI) mosaic (sol 1283 [sol—Mars solar day], image ccam02283) covering a prominent butte in the stratified layered sulfate-bearing unit (LSu) of Mount Sharp, Mars (see context in Fig. 2A). (B–D) Closeups of erosion-resistant outcrops from other RMI acquisitions (B,C: sol 1878, ccam04877; D: sol 2640, ccam05640) show sections of variably massive (i.e., massive with occasional finely bedded texture, in yellow) and heterolithic facies (sequences of weathered recessive sheets and resistant tabular bodies, in light blue). (E) Tracings using RMI images show bedding (red) and wedged, well-bedded, erosion-resistant outcrops hypothesized to represent sandstone bodies (shaded gray area). Tracings also include interpreted channel boundaries (green). Geometry of the lowermost erosion-resistant vertically stacked body (*) is typical of levee deposits: wing shape that thins away from channel cutbank, with facies grading laterally from variably massive to heterolithic (see also larger RMI images in Fig. S7 [see footnote 1]). (F) High Resolution Imaging Science Experiment (HiRISE) map with bedding as observed throughout the LSu. Dotted lines (numbered 1 to 4) mark boundaries between resistant and recessive intervals visible on RMI images (A) and reported on HiRISE, representing vertical passage between light and dark flooding surfaces; i.e., time lines. Blue reticles represent reference boulders located precisely on both RMI and HiRISE images. Red lines show image boundaries, and arrow points toward the Curiosity rover location.

accreted vertically, would be consistent with expectations about ancient Mars' environment: (1) sediment accommodation was not related to subsidence; and (2) overbank deposits were not stabilized, i.e., no vegetation was present.

CONCLUDING REMARKS

This set of ground-based outcrop observations provides enough elements in the LSu stratigraphy to propose a model for the evolution of depositional environments along the future rover traverse up Mount Sharp (Table S1 in the Supplemental Material). Lacustrine mudstones present in the Murray formation transition to vast accumulation in dry aeolian systems at or below the lowest interval of the LSu stratigraphy. The marker bed then records a prominent dune-field contraction and regional cessation of aeolian deposition, probably associated with water-table fluctuations. Further upsection, stratal architectures and textures reflect the resumption of a wetter climate.

The nature of sulfate enrichment in the unit cannot be specified by our remote analysis, but its presence is consistent with the proposed model. Primary or early diagenetic sulfate salts have already been identified in heterolithic members of the Murray formation (Kah et al., 2018; Rapin et al., 2019), which supports that sulfate was present in water feeding into the ancient Gale crater basin. The fluctuation between wet and dry climates implies oscillations of the water table, which would likely have triggered salt crystallization in sediment pore space (Milliken et al., 2014).

Evidence for environmental fluctuations has already been observed in the Murray formation (Hurowitz et al., 2017; Edgar et al., 2018; Stein et al., 2018; Rapin et al., 2019) but at a smaller scale compared to the hundreds of meters of the LSu thickness. As a whole, instead of an alkaline-to-acid or wet-to-dry unidirectional climate transition suggested by mineralogical signatures (Bibring et al., 2006; Milliken et al., 2010), our model predicts high-order fluctuations with several transitions between sustained wetter and drier climates recorded in Gale crater's Hesperian stratigraphy.

ACKNOWLEDGMENTS

Rapin and Ehlmann were supported by a NASA Mars Science Laboratory (MSL) Participating Scientist grant to Ehlmann. The work of Dromart was supported by Centre National d'Etudes Spatiales (CNES) through the ChemCam Program. Data used are available in the NASA Planetary Data System (<https://pds.nasa.gov/>). The MSL project is supported by the NASA Mars Exploration Program and CNES. We thank K.M. Stack, M. Pondrelli, A. Owen, and one anonymous reviewer for help in improving this manuscript.

REFERENCES CITED

- Bennett, K.A., and Bell, J.F., 2016, A global survey of martian central mounds: Central mounds as remnants of previously more extensive large-scale sedimentary deposits: *Icarus*, v. 264, p. 331–341, <https://doi.org/10.1016/j.icarus.2015.09.041>.
- Bibring, J.-P., et al., 2006, Global mineralogical and aqueous Mars history derived from OMEGA/Mars Express data: *Science*, v. 312, p. 400–404, <https://doi.org/10.1126/science.1122659>.
- Bradley, R.W., and Venditti, J.G., 2017, Reevaluating dune scaling relations: *Earth-Science Reviews*, v. 165, p. 356–376, <https://doi.org/10.1016/j.earscirev.2016.11.004>.
- Edgar, L.A., et al., 2018, Shaler: In situ analysis of a fluvial sedimentary deposit on Mars: *Sedimentology*, v. 65, p. 96–122, <https://doi.org/10.1111/sed.12370>.
- Fraeman, A.A., Ehlmann, B.L., Arvidson, R.E., Edwards, C.S., Grotzinger, J.P., Milliken, R.E., Quinn, D.P., and Rice, M.S., 2016, The stratigraphy and evolution of lower Mount Sharp from spectral, morphological, and thermophysical orbital data sets: *Journal of Geophysical Research: Planets*, v. 121, p. 1713–1736, <https://doi.org/10.1002/2016JE005095>.
- Gasnault, O., 2016, Imaging at long distance with ChemCam Remote Micro-Imager onboard MSL: Abstract 2329 presented at 47th Lunar and Planetary Science Conference, The Woodlands, Texas, 21–25 March.
- Gibling, M.R., 2006, Width and thickness of fluvial channel bodies and valley fills in the geological record: A literature compilation and classification: *Journal of Sedimentary Research*, v. 76, p. 731–770, <https://doi.org/10.2110/jsr.2006.060>.
- Grotzinger, J.P., et al., 2015, Deposition, exhumation, and paleoclimate of an ancient lake deposit, Gale crater, Mars: *Science*, v. 350, aac7575, <https://doi.org/10.1126/science.aac7575>.
- Grotzinger, J.P., and Milliken, R.E., eds., 2012, *Sedimentary Geology of Mars: SEPM (Society for Sedimentary Geology) Special Publication 102*, 270 p., <https://doi.org/10.2110/pec.12.102>.
- Grotzinger, J.P., et al., 2012, Mars Science Laboratory Mission and science investigation: *Space Science Reviews*, v. 170, p. 5–56, <https://doi.org/10.1007/s11214-012-9892-2>.
- Hurowitz, J.A., et al., 2017, Redox stratification of an ancient lake in Gale crater, Mars: *Science*, v. 356, eaah6849, <https://doi.org/10.1126/science.aah6849>.
- Kah, L.C., Stack, K.M., Eigenbrode, J.L., Yingst, R.A., and Edgett, K.S., 2018, Syndepositional precipitation of calcium sulfate in Gale Crater, Mars: *Terra Nova*, v. 30, p. 431–439, <https://doi.org/10.1111/ter.12359>.
- Kirk, R.L., et al., 2008, Ultrahigh resolution topographic mapping of Mars with MRO HiRISE stereo images: Meter-scale slopes of candidate Phoenix landing sites: *Journal of Geophysical Research*, v. 113, E00A24, <https://doi.org/10.1029/2007JE003000>.
- Kocurek, G., 1988, First-order and super bounding surfaces in eolian sequences—Bounding surfaces revisited: *Sedimentary Geology*, v. 56, p. 193–206, [https://doi.org/10.1016/0037-0738\(88\)90054-1](https://doi.org/10.1016/0037-0738(88)90054-1).
- Le Deit, L., Hauber, E., Fueten, F., Pondrelli, M., Rossi, A.P., and Jaumann, R., 2013, Sequence of infilling events in Gale Crater, Mars: Results from morphology, stratigraphy, and mineralogy: *Journal of Geophysical Research: Planets*, v. 118, p. 2439–2473, <https://doi.org/10.1002/2012JE004322>.
- Le Mouélic, S., et al., 2015, The ChemCam Remote Micro-Imager at Gale crater: Review of the first year of operations on Mars: *Icarus*, v. 249, p. 93–107, <https://doi.org/10.1016/j.icarus.2014.05.030>.
- Le Mouélic, S., 2019, Correction of stray light in ChemCam Remote Micro-Imager long distance images: Abstract 1399 presented at 50th Lunar and Planetary Science Conference, The Woodlands, Texas, 18–22 March.
- Loope, D.B., 1985, Episodic deposition and preservation of eolian sands: A late Paleozoic example from southeastern Utah: *Geology*, v. 13, p. 73–76, [https://doi.org/10.1130/0091-7613\(1985\)13<73:EDAPOE>2.0.CO;2](https://doi.org/10.1130/0091-7613(1985)13<73:EDAPOE>2.0.CO;2).
- Mauz, B., Hijma, M.P., Amorosi, A., Porat, N., Galili, E., and Bloemendal, J., 2013, Aeolian beach ridges and their significance for climate and sea level: Concept and insight from the Levant coast (East Mediterranean): *Earth-Science Reviews*, v. 121, p. 31–54, <https://doi.org/10.1016/j.earscirev.2013.03.003>.
- Milliken, R.E., Grotzinger, J.P., and Thomson, B.J., 2010, Paleoclimate of Mars as captured by the stratigraphic record in Gale Crater: *Geophysical Research Letters*, v. 37, L04201, <https://doi.org/10.1029/2009GL041870>.
- Milliken, R.E., Ewing, R.C., Fischer, W.W., and Hurowitz, J., 2014, Wind-blown sandstones cemented by sulfate and clay minerals in Gale Crater, Mars: *Geophysical Research Letters*, v. 41, p. 1149–1154, <https://doi.org/10.1002/2013GL059097>.
- Powell, K.E., Arvidson, R.E., and Edwards, C.S., 2019, Spectral properties of the layered sulfate-bearing unit in Mount Sharp, Gale Crater, Mars: Abstract 1455 presented at 50th Lunar and Planetary Science Conference, The Woodlands, Texas, 18–22 March.
- Rapin, W., et al., 2019, An interval of high salinity in ancient Gale crater lake on Mars: *Nature Geoscience*, v. 12, p. 889–895, <https://doi.org/10.1038/s41561-019-0458-8>.
- Rubin, D.M., and Carter, C.L., 2006, *Cross-Bedding, Bedforms, and Paleocurrents (second edition): SEPM (Society for Sedimentary Geology) Concepts in Sedimentology and Paleontology 1*, 187 p., <https://doi.org/10.2110/csp.87.01>.
- Scherer, C.M.S., 2000, Eolian dunes of the Botucatu Formation (Cretaceous) in southernmost Brazil: Morphology and origin: *Sedimentary Geology*, v. 137, p. 63–84, [https://doi.org/10.1016/S0037-0738\(00\)00135-4](https://doi.org/10.1016/S0037-0738(00)00135-4).
- Stack, K.M., Grotzinger, J.P., and Milliken, R.E., 2013, Bed thickness distributions on Mars: An orbital perspective: *Journal of Geophysical Research: Planets*, v. 118, p. 1323–1349, <https://doi.org/10.1002/jgre.20092>.
- Stack, K.M., et al., 2018, Evidence for plunging river plume deposits in the Pahrump Hills member of the Murray formation, Gale crater, Mars: *Sedimentology*, v. 66, p. 1768–1802, <https://doi.org/10.1111/sed.12558>.
- Stein, N., et al., 2018, Desiccation cracks provide evidence of lake drying on Mars, Sutton Island member, Murray formation, Gale Crater: *Geology*, v. 46, p. 515–518, <https://doi.org/10.1130/G40005.1>.

Printed in USA